FAILURE MODES AND DAMAGE PROGRESSION OF A QUASI-ISOTROPIC GRAPHITE-EPOXY COMPOSITES IN FLEXURAL BENDING TEST

Echaabi, J., Trochu, F., Ratle, A., Gauvin, R.
Mechanical Engineering, École Polytechnique,
C.P. 6079, Succ."Centre ville", Montréal, Qué., Canada, H3C 3A7
Telephone (514) 340-4280, Fax (514) 340-5867

ABSTRACT

Predicting failure stress and failure modes in composite laminates is very difficult. The choice between failure criteria is complex and there is a lack of experimental study to validate the results obtained. In this paper, an experimental study of damage progression and failure modes of graphite-epoxy laminates in three point bending tests is presented. A quasi-isotropic $[(\pm45/90/0)_3]_s$ graphite-epoxy composite is investigated. C-Scan method and microscopic sectioning permit to monitor damage progression and failure modes during the experiment. Specimens at different failure levels are used to determine failure succession and the effect of geometrical parameters on the successive failures and on the failure modes is studied.

INTRODUCTION

Advanced composites laminates reinforced with continuous fibres exhibit a large diversity of failure behaviours. Consequently a great number of failure criteria have been used to describe the failure envelopes of these materials [1,2]. Up till now more failure criteria are still being published [3,4,5]. A few models which incorporate the failure modes in the equation of the criterion have been proposed [6,7,8]. Each of these failure criteria is validated on a particular experimental data. These data are obtained by running biaxial tests which are difficult to perform, not reliable and present a large scatter [2,7]. Moreover, the effect of failure modes on the failure stresses or strains is not well-known. There is a lack of experimental data on failure modes to validate theoretical failure criteria. This work presents an experimental procedure to investigate damage progression and failure modes in a graphite-epoxy laminates in flexural bending tests.

EXPERIMENTAL PROCEDURE

Preparation of specimens

The laminate staking sequence used in this work is $[(\pm45/90/0)_3]_s$. Each specimen was originally cut from a 16 x 16 cm plate. A large wide of different specimens have been studied as shown in Table 1. The number of specimens used to investigate damage progression is different for each type of specimen characteristics.

Table 1. Specimens characteristics

Laminates	Width (W) (mm)	Span (ℓ) (mm)	Length (L) (mm)	Thickness (T) (mm)	ℓ/T
A	25	57.5	75	3,6	16
B	25	115.0	150	3,6	32
C	25	136.5	150	3,6	38
D	10	57.5	75	3,6	16
E	10	115	150	3,6	32
F	10	136	150	3,6	38

The side edge of the specimens was polished with 5 and 0.5 micron polishing powder in order to facilitate microscopic investigation and to prevent damage induced during the cutting process. The dimensions of the specimens are in accord with ASTM specification D790 [9]. MTS loading machine equipped with a PC is used. The load displacement curves are recorded automatically. The experimental setup is shown in Fig.1.

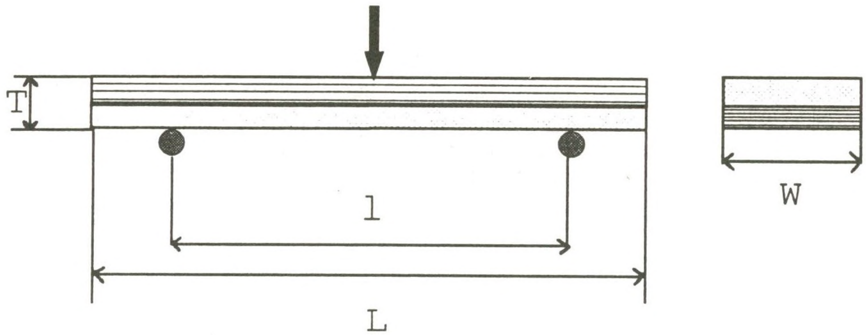

Figure 1. Experimental setup

Damage progression is monitored by C-Scan and microscopic investigation. C-Scan analysis is used before the first failure occurs.

Test procedure

For each set of geometrical parameters four specimens were cut and polished. For some specimens ultrasonic scanning is used before and after preparation to ensure that they are free of cutting damages.

A first specimen is used to obtain the macroscopic curve load vs displacement. This permits to determine the succession of failures. A second specimen is loaded to a given displacement before the first failure. C-Scan analysis and microscopic investigation are used to detect matrix cracking in this specimen. The other specimens are used to monitor damage progression and the failure modes before and after the successive failures. Only microscopic investigation is used to perform this tasks.

RESULTS AND DISCUSSION

Span to depth ratio effect

Fig. 2 shows macroscopic curves obtained for A, B and C specimens. Each curve is obtained for a given span-to-depth ratio (ℓ/T). For specimens A ($\ell/T = 16$) four successive failures are obtained whereas for specimens B and C (respectively $\ell/T = 32$ and 38) only one macroscopic failure is observed.

Fig. 3 shows other macroscopic curves for specimens D, E, F (respectively $\ell/T = 16$, 32 and 38). With respect to specimens A, B and C, only the width is different. Specimen D presents only two successive failures and specimens E, F one macroscopic failure. Successive failures depend strongly on span-to-depth ratio (ℓ/T) and also on the specimen width.

The main objective of this work is to investigate damage progression and successive failure. The macroscopic curves shown in the above section indicate that some specimens present successive failures whereas the others exhibit a unique catastrophic failure. In the sequel the damage mechanism in the specimens with successive failures will be investigated.

Successive failures

As shown in Fig. 2, type A specimen presents successive failures. The displacement at first failure is 3.88 mm. In order to monitor matrix cracking before the first failure, other specimens of the same type are loaded respectively up to 1.5 and 2.5 mm. Fig. 4 presents the C-Scan images before and after the specimen were loaded. This figure indicates that damage has occurred in the two specimens. Microscopic investigation is used to determine the nature and the location of the damage.

The results obtained with microscopic investigation for the two specimens are shown in Fig. 5. Matrix cracking appears first in the plies 90° for a displacement 1.5 and grows to the plies $\pm 45°$ for a displacement of 2.5 mm. A comparison between C-Scan image and microscopic investigation for specimen A shows that the C-Scan detects matrix cracking in the specimen.

Another type A specimen is loaded up to first failure. Only microscopic investigation can be used. For this specimen fiber failure is observed in the 0° plies as shown in Fig. 6. Also appear in the same figure specimens after the second failures.

For this type of specimens, the sequence of failure is as follows. The first cracks appear in the matrix at the lower 90° ply and grow to the plies ±45. The first fiber failure appear in the two lower 0° plies and is preceded by matrix cracking in the second series of plies 90° and ±45 from the bottom as shown in Fig. 5(c). The first failure in Fig. 2 corresponds to failure of the eight plies [±45/90/0/±45/90/0]. The second failure corresponds to failure of the two 0° plies in the plane of symmetry. The failure initiates at the bottom and grows to the top. Failure of ±45 and 90° has no significant effect on the macroscopic failure. Failure of type A specimens is fiber dominated.

For the second series of specimens (D), only the width is different and equal to 10 mm. The load vs displacement curve is shown in Fig. 3. Two successive failures are observed. Since the staking sequence is the same, failure mechanism is different in this case but the same procedure used before will permit to monitor damage progression.

CONCLUSION

The effect of geometrical parameters on the failure behaviour of a graphite-epoxy laminated beam under static testing condition has been studied. Damage progression has been monitored and characterized for different geometrical parameters of the specimens. Also the failure mode at each step of deformation are known. These results will permit to validate failure criteria particularly beyond the first failure.

REFERENCES

1. M.N. NAHAS, Survey of failure and postfailure theories of laminated fiber reinforced composites, Jour. Comp. Tech. & Research, Vol. 8, p. 138-153 (1986).

2. R.E. ROWLAND, Strength theories and their experimental correlation, Handbook of composite, Vol. 3 (1986).

3. L.J. HART-SMITH, How to calculate in plane strength of fiber-polymer composite laminate, Sampe Journal, Vol. 28, No. 6 (1992).

4. W. MICKAELI and J. HAYBRECHTS, A new approach for the dimensioning of thick laminates using physically based strength criteria, 39th Sampe Symposium, April 11-14 (1994).

5. J. ECHAABI, F. TROCHU, and R. GAUVIN, A general strength theory for composite materials based on dual kriging interpolation, Jour. Reinf. Plast. Comp., to appear.

6. Z. HASHIM, Failure criteria for unidirectional fiber composites, Jour. Appl. Mechanics, Vol. 47, p. 329-334 (1980).

7. J. ECHAABI, F. TROCHU, and R. GAUVIN, An evolutive method to predict strength of composite laminates, ATMAM, Montréal, Québec, Canada (1994).

8. W.W. FENG, A failure criterion for composite materials, Jour. Comp. Mater., Vol. 25 (1991).

9. ASTM test D790, American standards of testing and materials, Vol. 801 (1992).

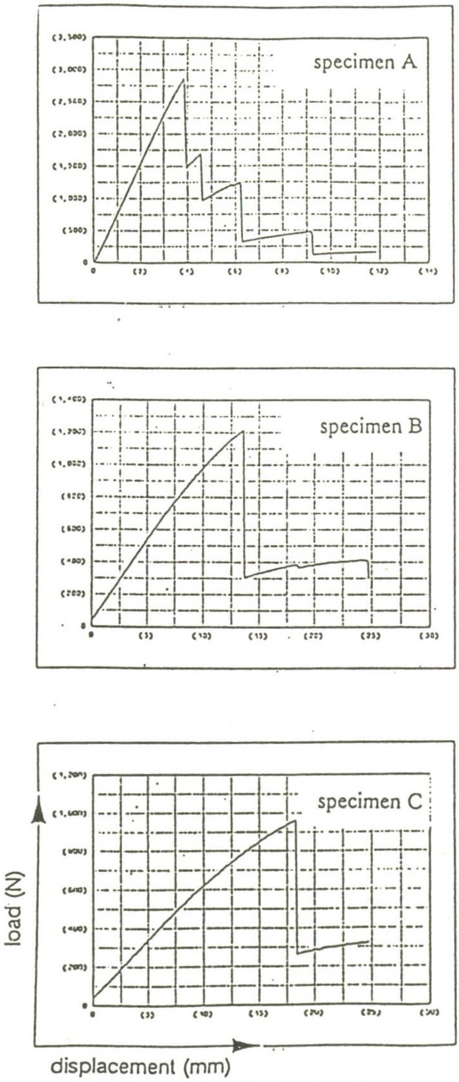

Figure 2. Load vs displacement for A, B and C specimens.

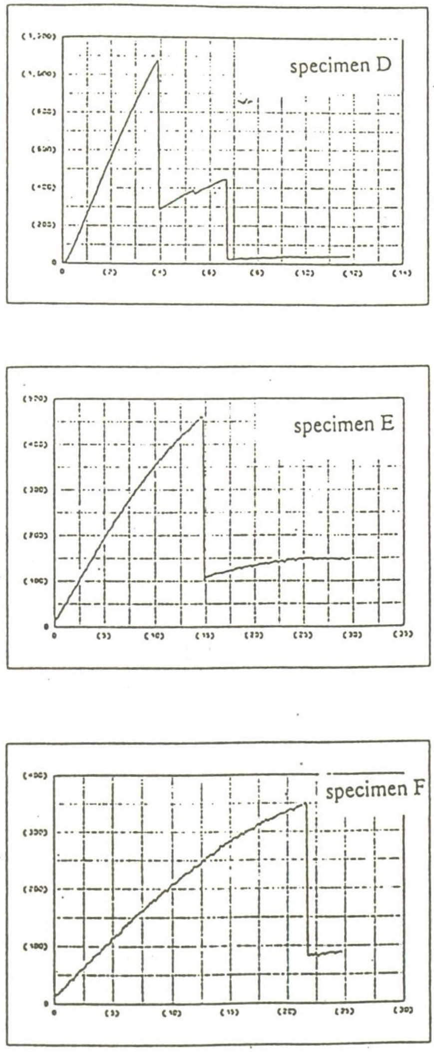

Figure 3. Load vs displacement for D, E and F specimens.

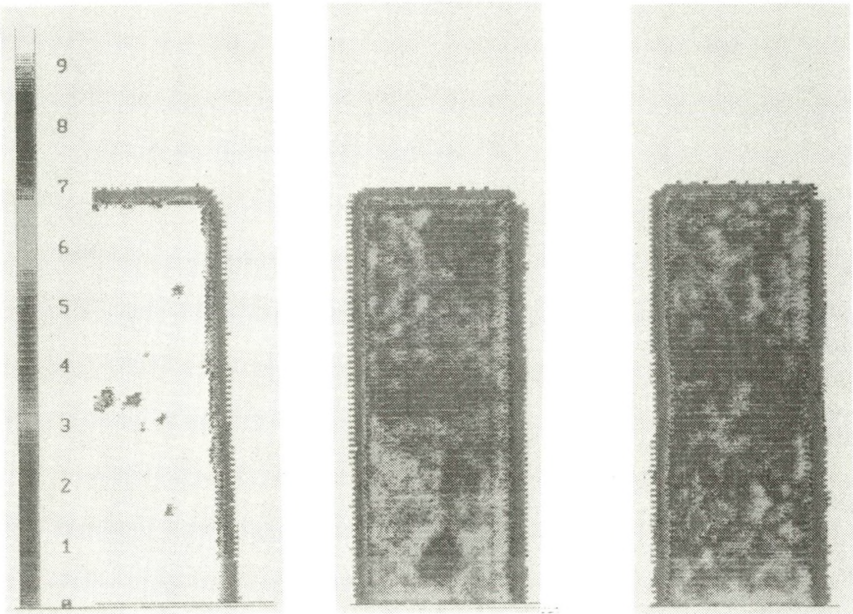

a) virgin specimen b) loaded up to 1.5 mm c) loaded up to 2.5 mm

Figure 4. Specimen C-scan image before and after loading.

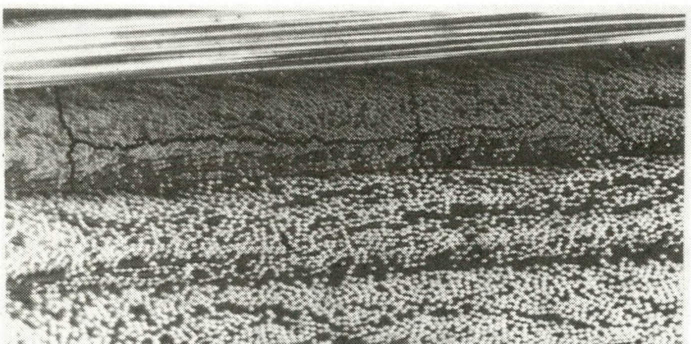

a) Cracks in the 90° ply in the specimen loaded up to 1.5 mm.

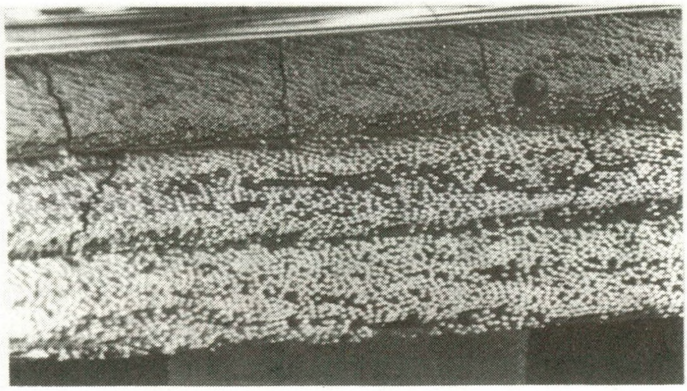

b) Cracks in 90° and 45° in the specimen loaded up to 2.5mm.

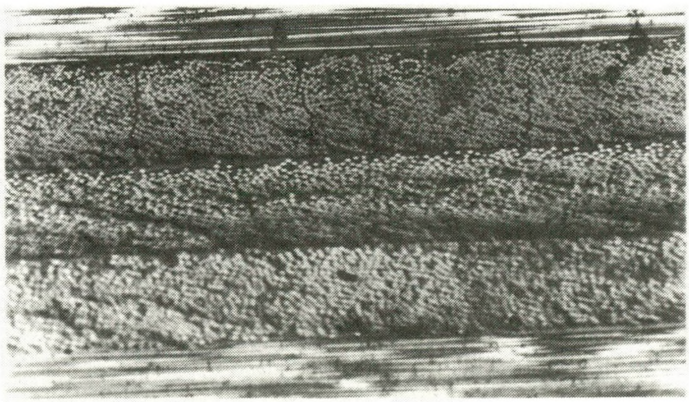

c) Cracks in 90° and 45° plies in the second sequence of [+/-45/90/0] before first failure.

Figure 5. Photomicrographs showing development of cracks under static loading.

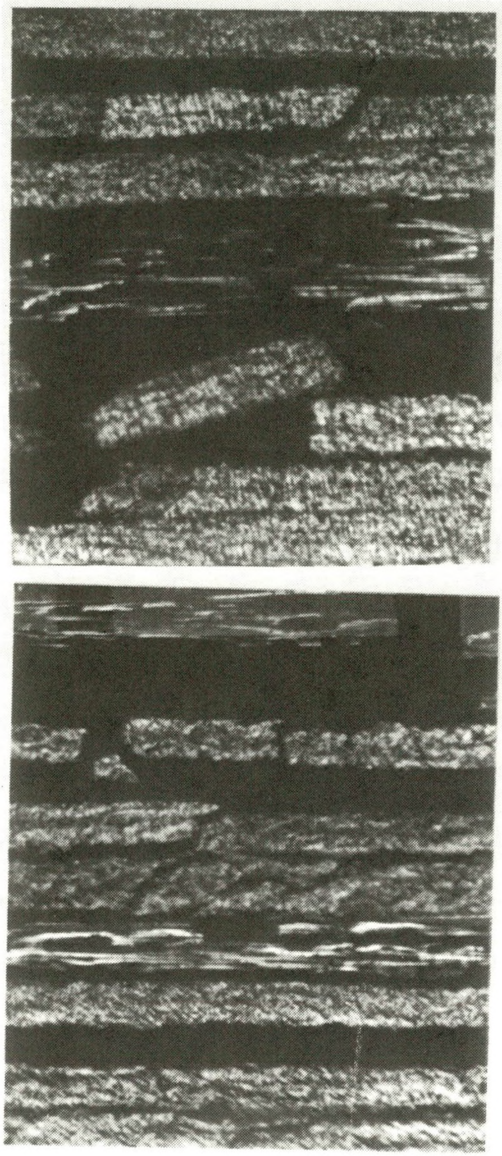

figure 6. Photomicrographs showing specimen after first and second failure.